

Nature of Surface-Induced Nuclear-Spin Relaxation of Gaseous He³ †

W. A. Fitzsimmons,* L. L. Tankersley, ‡ and G. K. Walters

Department of Physics, Rice University, Houston, Texas 77001

(Received 19 September 1968)

Surface-induced spin-lattice relaxation times are reported as a function of temperature for gaseous He³ in glass containers. The results are interpreted in terms of a phenomenological theory incorporating distinctly different relaxation processes at low and high temperatures, respectively. The low-temperature mechanism involves He³ adsorption on the glass surface, while the high-temperature mechanism (applicable to Pyrex and quartz surfaces) involves permeation of He³ into the container material. The latter mechanism can be eliminated by using relatively impermeable aluminosilicate glass containers, and the resulting He³ nuclear-spin relaxation times become quite long (>10⁵ sec) at low gas densities and moderate temperatures. Preliminary experiments using aluminosilicate containers suggest that spin exchange with optically pumped rubidium vapor may lead to sizeable He³ nuclear polarization at relatively high densities; in these experiments a He³ nuclear-spin relaxation time approaching 10⁶ sec was observed at 100°C in a 500-Torr He³ sample containing rubidium vapor. Phenomenological theory suggests that spin-lattice and spin-spin relaxation times are equal for adsorption-controlled relaxation.

I. INTRODUCTION

Interactions of fluid atoms with their containing walls have long been known to play a significant role in nuclear- and electron-spin relaxation of gases and liquids. For electron spins, considerable progress has been made toward an understanding of the mechanisms involved, particularly through buffer-gas-free optical-pumping studies of alkali atoms interacting with hydrocarbon surfaces,¹ and by using the atomic hydrogen maser to study hydrogen spin relaxation at the maser storage bulb walls.²

In contrast, the mechanisms for surface-induced relaxation of nuclear spins have remained relatively obscure. In some cases, coupling of gas-atom nuclear spins to identifiable surface paramagnetic centers has been demonstrated by dynamic spin-pumping experiments.³ However, the analysis of such experiments invariably suggests the presence of other unknown competing relaxation processes, presumably due to surface paramagnetic centers other than those involved in spin pumping.⁴

The surface relaxation behavior of He³ nuclei in both liquid and gas phases is particularly enigmatic. Surface relaxation in liquid He³, for example, has been found to depend on the surface composition and preparation, but does not correlate with the apparent density of paramagnetic centers on the surface.⁵ Furthermore, liquid He³ dynamic polarization schemes relying on coupling to surface paramagnetic centers have proven to be categorical failures.⁶ In the case of gaseous He³, evidence of very effective surface relaxation processes at low temperatures has been

found by Walters,⁵ Luszczynski *et al.*,⁷ and McAdams.⁸

By virtue of its ¹S₀ electronic structure, its chemical inertness, and the very long intrinsic spin relaxation times expected in the gas phase, the spin $\frac{1}{2}$ He³ nucleus represents perhaps the simplest available probe for the study of nuclear relaxation during collisions with solid surfaces. In the experiments reported here, the temperature and magnetic field dependence of the surface-induced He³ nuclear-spin-lattice relaxation time was measured for low-density samples of He³ gas contained in sealed glass vessels.⁹ Optical-pumping techniques provide a particularly simple and direct means for determining He³ relaxation times. The procedure used was to first optically induce a large (~10%) nuclear polarization¹⁰ in the sample, then to monitor the decay of the polarization toward its thermal-equilibrium value using a conventional nuclear-magnetic resonance method.

The container materials studied included Pyrex, quartz, and two types of aluminosilicate glasses. The results are interpreted in terms of He³ adsorption at the container surface, and, in the cases of Pyrex and quartz, permeation into the bulk of the container material.

The very long He³ relaxation times (>10⁵ sec) observed at moderate temperatures for the aluminosilicate containers suggests that the optical pumping of rubidium vapor using He³ as the buffer gas may now be a feasible method for obtaining significant nuclear polarizations in dense samples of He³. Previous attempts to orient He³ nuclei in this way have failed to yield significant polarization because the Rb-He³ spin-exchange time

(typically 10^6 to 10^7 sec) was much longer than the He^3 surface-induced spin relaxation time ($T_1 \sim 2 \times 10^3$ sec).¹¹ However, using aluminosilicate glasses, we find T_1 to be increased to nearly 10^6 sec, and a corresponding increase in the He^3 polarization is observed.

II. EXPERIMENTAL PROCEDURE

The gaseous He^3 samples were contained in spherical bulbs, approximately 5 cm in diameter, blown from several glasses – Pyrex, supracil quartz, and Corning 1720 and 1723 aluminosilicates. The containers were subjected to identical cleaning procedures starting with degreasing in strong laboratory detergent and thorough rinsing in distilled water. Then they were installed on a Pyrex vacuum and gas-handling system, evacuated to a pressure of 10^{-7} Torr at 800°K and filled to 1 Torr with a helium-hydrogen mixture in which an intense electrical discharge was ignited for about 30 min. After the discharge cleaning each vessel was evacuated again, baked out, and filled to the desired He^3 density through a copper-foil cold trap immersed in liquid helium. Finally, the bulbs were tipped off to yield permanently sealed samples with He^3 densities varying from 2 to 20 Torr at room temperature.

A single 500-Torr sample containing a small quantity of rubidium (natural isotopic mixture) was prepared in a Corning 1723 container for the rubidium experiment described in Sec. V.

He^3 nuclear-spin-lattice relaxation times (T_1) were measured by a nuclear-magnetic resonance method over a temperature interval from 55 to 350°K . The experiment may be described with reference to Fig. 1. The basic components of the apparatus are:

- (1) The optical-pumping system to initially polarize the He^3 gas.
- (2) A nuclear-magnetic resonance spectrometer to detect and monitor the decay of the He^3 nuclear polarization.
- (3) A cryogenic system to control the temperature of the sample.

The glass bulb containing the He^3 sample is placed in a Dewar with flat windows on the bottom. The windows provide an optical path for the circularly polarized $1.08\text{-}\mu$ optical-pumping radiation emitted by a bright He^4 discharge lamp. The pumping radiation is incident on the He^3 along the direction of an external magnetic field provided by a coaxial end-corrected solenoid. A weak electrodeless discharge ignited in the He^3 populates the 2^3S_1 metastable state and the metastable atoms become polarized via the absorption of the pumping radiation. Excitation-transfer collisions between the metastable atoms and ground-state atoms transfer the optically induced spin polarization to the ground-state nuclei in a manner

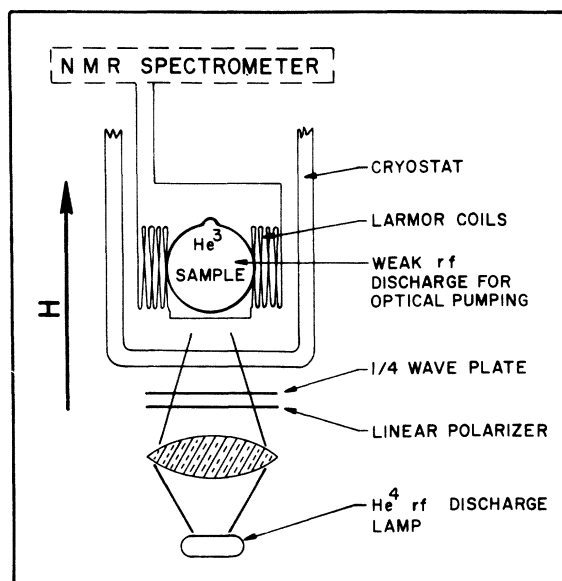


FIG. 1. Schematic diagram of apparatus used in He^3 surface-induced nuclear-spin relaxation studies.

described by Colegrove, Scheerer, and Walters.¹² Ground-state polarizations between 5 and 15% are typical. After the sample is polarized, both the discharge in the sample and the pumping lamp are turned off for the remainder of the experiment and the decay of the nuclear polarization is monitored periodically by a slow-passage NMR technique. Larmor coils wound around the sample form one arm of a twin- T bridge. An rf generator operated at a frequency of 735 kHz and a radio receiver complete the magnetic-resonance circuit. The large optically induced initial polarization assures a good signal-to-noise ratio over periods long compared to T_1 .

The external magnetic field of approximately 225 G provided by a fourth-order end-corrected solenoid was homogenous to a few parts in 10^4 over the sample volume of approximately 70 cm^3 . In these experiments good field homogeneity is important since the He^3 nuclear polarization can be destroyed by gradients in the external magnetic field.¹³ This effect will be discussed later.

Since the measured relaxation times were often very long, a means for introducing a standard signal was devised in order to correct for the day-to-day drift in the over-all sensitivity of the spectrometer. The standard signal was generated by switching a very small fixed capacitor into the resistive side of the NMR bridge. Such a capacitor unbalances the bridge in a manner electrically equivalent to the unbalance caused by the nuclear-resonance absorption.

An important experimental requirement is temperature stability of the sample, at somewhat inconvenient temperatures, over time periods of

TABLE I. Properties of cryogenic fluids covering the temperature range from 277 to 63°K. (Freon properties taken from "Physical Properties of Freon Family of Fluorocarbon Compounds" E. I. du Pont de Nemours & Co. Technical Bulletin B-2).

	Freon 114	Freon 12	Freon 13	Freon 14	Argon	Nitrogen
Boiling point at 1 atm (°K)	277	243	192	145	87	77
Freezing point (°K)	179	115	92	89	84	63
Density of liquid (g/cc)	1.46	1.31	1.30	1.32	1.39	0.81
Heat of vaporiza- tion at bp (cal/g)	32.5	39.5	35.5	32.5	37.6	47.6

2 or 3 days. A set of commercially available nontoxic fluorocarbon compounds (Freons) span most of the desired temperature range. The pertinent physical properties of these fluorocarbons are shown in Table I. Liquid nitrogen and liquid argon were used also and their properties are included for comparison. Temperature control of the sample is achieved in the standard way by immersing the sample in the cryogenic fluid, and regulating the fluid vapor pressure (hence temperature) by pumping.

The fluorocarbon compounds are readily available in the form of liquids or compressed gases that can be easily liquefied at atmospheric pressure with the apparatus shown in Fig. 2. The liquefaction Dewar is initially evacuated to remove any residual air and, depending upon the Freon to be liquefied, the metal can is filled with

either liquid nitrogen or dry ice and acetone. The cooling of the gas upon expansion, followed by contact with the cold metal surface in the Dewar results in liquefaction rates of roughly 2 liters/h. The use of cryogenic fluids with vapor pressure regulation resulted in temperature stability of $\pm 1^\circ\text{K}$ over a 2-day period. Temperatures were monitored with a thermocouple attached to the sample container.

Temperatures higher than room temperature were achieved by circulating hot water through copper coils thermally connected to the sample by a silicone fluid. Temperature stability for this method was $\pm 3^\circ\text{K}$ over a 3-day period.

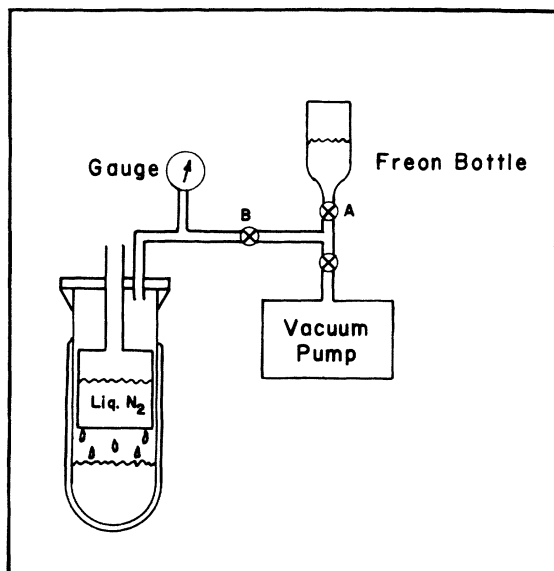


FIG. 2. Schematic diagram of apparatus used to liquefy fluorocarbon compounds.

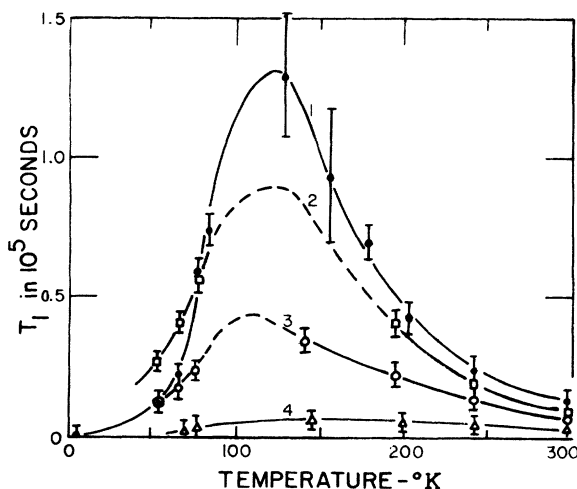


FIG. 3. Surface-induced He^3 nuclear-spin relaxation times versus temperature for Pyrex and quartz surfaces. Curves 1, 2, and 3 represent measurements on three samples in different Pyrex containers with He^3 pressures at room temperature of 10, 20, and 20 Torr, respectively. Curve 4 represents the data taken on a single 10-Torr sample in a fused quartz container.

III. EXPERIMENTAL RESULTS AND INTERPRETATION

The experimental results for the surface-induced He³ nuclear-spin relaxation time T_1 as a function of temperature are shown in Fig. 3 for Pyrex and quartz surfaces. Three curves for Pyrex containers are shown to indicate the variation in absolute magnitude of the measured relaxation times from sample to sample. These variations are attributed to differences of an unknown nature in surface conditions from one sample to the next. No systematic dependence of the relaxation time on He³ density was observed over the density range corresponding to 2 to 20 Torr at room temperature. This is to be expected for surface relaxation since the rate of wall collisions per atom is independent of density.¹⁴ Measurements on a given sample are reproducible, indicating that there are no significant effects due to aging (up to 2 yr) or thermal cycling. The uncertainties in the measured relaxation times are typically 10 to 15%, and are determined principally by signal-to-noise limitations of the NMR spectrometer. The experimental errors tend to be greater for the very long relaxation times because of spectrometer and thermal drift.

The most interesting feature of the data shown in Fig. 3 is the characteristic relaxation-time maximum occurring for all samples near 125°K. This behavior suggests that distinctly different surface relaxation mechanisms are operative at low and high temperatures, respectively.

The probability of a He³ nuclear-spin flip during an atomic collision with the container wall should depend on the collision duration or sticking time. Therefore one is led to seek an explanation of the relaxation-time data in terms of the (presumably different) sticking mechanisms that predominate at low and high temperatures. The obvious candidates are adsorption due to van der Waals attraction at lower temperatures, and the well-known permeation of helium into Pyrex and quartz at higher temperatures.^{15,16} In the next section a quantitative phenomenological theory incorporating these ideas is developed and shown to be in good agreement with the experimental results.

The suggested high temperature, or permeation-dominated, relaxation mechanism was tested experimentally by preparing He³ samples in containers made of nearly impermeable aluminosilicate glasses (Corning 1720 and 1723). Norten¹⁵ and Altemose¹⁶ have shown that glasses composed of a high percentage of glass-forming oxides, or network formers (principally SiO₂), have a chain-like structure with openings large enough for small gas atoms to permeate; hence, quartz and Pyrex are relatively permeable to helium. In the aluminosilicate glasses, Al₂O₃ acts as a network modifier, with aluminum ions filling the openings in the glass network. As a consequence, Corning

1720 and 1723 aluminosilicate glasses are about three orders of magnitude less permeable to helium than is Pyrex (Corning 7740) at room temperature.

Nuclear-spin relaxation times measured for He³ samples in a number of aluminosilicate glass bulbs are shown in Fig. 4, along with a representative Pyrex curve for comparison. As with Pyrex and quartz containers, there is considerable – though reproducible – variation in T_1 from sample to sample, presumably indicating different microscopic surface areas or varying densities of surface paramagnetic centers that induce He³ nuclear-spin relaxation. With the exception of curve 5, it is clear that, in contrast to the results for Pyrex and quartz, there is no evidence of a T_1 maximum. This is regarded as strong experimental support for a permeation-controlled high-temperature relaxation mechanism in the cases of Pyrex and quartz surfaces. The observed He³ relaxation behavior for aluminosilicate surfaces is apparently adsorption-controlled at all accessible temperatures. The slight turnover of curve 5 at high temperatures is not due to any surface property but can be attributed to the magnetic-gradient relaxation mechanism described by Scheerer and Walters.¹³ For the gradients associated with the solenoid field used in these measurements, the calculated-gradient relaxation time is inversely proportional to

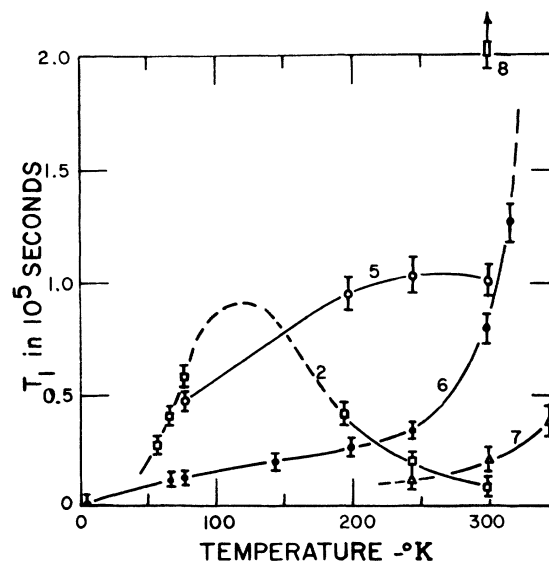


FIG. 4. Surface-induced He³ nuclear-spin relaxation time versus temperature for aluminosilicate surfaces. Curves 6 and 7 and the point labeled 8 represent data taken on three samples in different Corning 1723 containers. Curve 5 is data taken on a single Corning 1720 container. Curve 2 is representative Pyrex data included for comparison.

the square root of the temperature and is about 1 to 5×10^5 sec; the large uncertainty results from extreme sensitivity to the exact position of the sample in the solenoid, and to slight variations in bulb size and shape from sample to sample. It can be seen from Fig. 4 that the longer relaxation times are in the range where gradient effects are expected to become important. In an homogeneous magnetic environment, the relaxation times of samples 5 and 8 could be expected to be much longer at the higher temperatures than the values indicated in Fig. 4.

Supporting evidence for gradient-controlled relaxation at the higher temperatures is provided by the 10^6 sec relaxation time measured on a high-density (500 Torr at 373°K) He³ sample. The gradient relaxation time is directly proportional to density and does not contribute in our apparatus in the case of this sample. Studies of the high-density sample are reported in Sec. V.

An attempt was made to measure the surface relaxation time at 4.2°K in a few samples contained in Pyrex and in one sample contained in Corning 1723 aluminosilicate glass (curve 6 of Fig. 4). The optical-pumping method for producing the initial polarization will not work at low temperatures because the cross section for excitation transfer in collisions between metastable and ground-state He³ atoms approaches zero.¹⁷ Thus the experimental approach consisted of initially polarizing the sample at 77°K and then cooling it as quickly as possible in the hope that the polarization decay could be monitored at 4.2°K. In all attempts the time required to cool the sample to 4.2°K was 5 min or less, but no NMR signal was detected. This places an upper limit of about 2 min on the He³ surface relaxation time for all samples at 4.2°K.

The magnetic field dependence of surface-induced relaxation times was measured at several temperatures for He³ samples in both Pyrex and aluminosilicate containers. Because of the long relaxation times, it is a simple matter to monitor the polarization decay at any accessible field strength. This is accomplished by periodically adjusting the field to the 225-G value required for NMR, then quickly returning the field to the desired value, all in a time short compared with T_1 . The experimental results are shown in Fig. 5. The maximum magnetic field of 225 G is the highest the solenoid can produce without overheating. The lower-field limit of approximately 10 G was established to avoid relaxation due to gradients in the ambient laboratory field.

The magnetic field dependence of the surface-induced He³ nuclear-spin relaxation cannot be adequately interpreted at present because of the very limited information available on the details of the microscopic relaxation mechanism. It is probably safe to assume that the relaxing agents

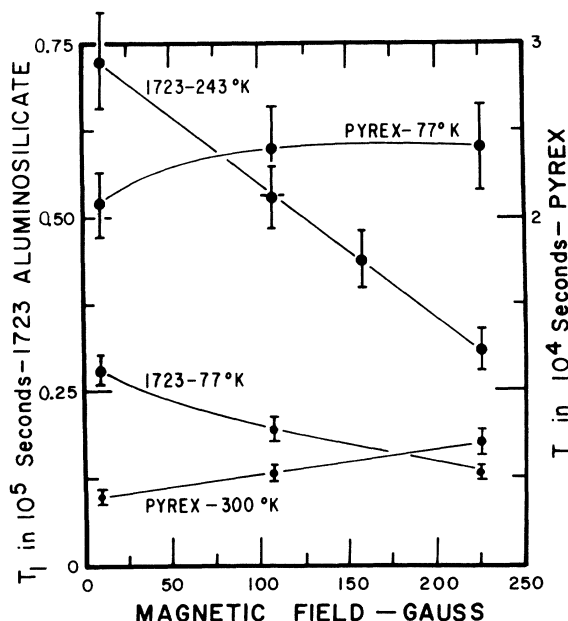


FIG. 5. Magnetic field dependence of surface-induced He³ nuclear-spin relaxation times. Curves are labeled according to surface material and temperature at which the measurements were made.

are paramagnetic centers on or near the glass container surface. However, these experiments provide no information on the nature of the paramagnetic ions, or on their locations in the glass network. About all that can be said about the magnetic field dependence of T_1 at this juncture is that it probably reflects a field dependence of the paramagnetic relaxation of the surface centers. A few additional comments on this subject are made in Sec. IV.

IV. PHENOMENOLOGICAL THEORY

The surface-induced relaxation behavior of gaseous He³ can be described quantitatively by consideration of the average collision duration (or sticking time) t_s characterizing the He³ surface interaction. A rather general expression relating the observed He³ relaxation time T_1 to t_s is first derived in a manner paralleling that of Korrington *et al.* in their treatment of magnetic spin pumping of fluids contained in porous media.⁴ The behavior of T_1 at low and high-temperature limits is then analyzed by evaluating t_s and the steady-state number n of He³ atoms under the influence of the surface, in terms of He³ adsorption and permeation properties, respectively.

A. Basic Equations

Consider a sample of N He³ atoms in a con-

tainer of volume V and surface area A . The relatively small number n of these atoms interacting with the container surface at any instant can be regarded as continually interchanging at the rate n/t_s with atoms of the bulk gas. If T_s is the characteristic relaxation time for the atoms under the influence of the surface, then the rate equations describing the relaxation of an initially polarized sample are

$$\frac{dn_+}{dt} = -\frac{1}{2T_s} (n_+ - n_-) - \frac{1}{Nt_s} (n_+N_- - n_-N_+), \quad (1a)$$

$$\frac{dN_+}{dt} = \frac{1}{Nt_s} (n_+N_- - n_-N_+), \quad (1b)$$

where the intrinsic relaxation in the bulk gas and the small population differences due to the thermal Boltzmann factor are neglected. N_+ and N_- are the numbers of He³ atoms in the gas with magnetic quantum numbers $m = +\frac{1}{2}$ and $-\frac{1}{2}$, respectively; n_+ and n_- are the corresponding quantities for the atoms interacting with the surface. Equations (1) can be rewritten in terms of the gas and surface atom polarizations, $P = (N_+ - N_-)/N$ and $p = (n_+ - n_-)/n$, using $N_+ + N_- = N$ and $n_+ + n_- = n$:

$$dp/dt = -p/T_s - (p - P)/t_s \quad (2a)$$

$$dP/dt = (n/N)(p - P)/t_s. \quad (2b)$$

The solutions of Eq. (2) are of the form $P = a_i \times \exp(-\lambda_i t)$ and $p = \beta_i \exp(-\lambda_i t)$. Using $n \ll N$, the rate constants λ_i are

$$\lambda_1 = 1/T_s + 1/t_s + n/Nt_s, \quad (3a)$$

$$\lambda_2 = n/N(t_s + T_s). \quad (3b)$$

The decay to zero of the observable polarization P from its large initial value is characterized by the slower rate λ_2 . Thus

$$T_1 = (N/n)(t_s + T_s) \text{ for } n \ll N. \quad (4)$$

This expression for T_1 has been derived without reference to a specific atom-surface interaction and is therefore a suitable point of departure for the discussion of particular models of surface relaxation. The quantities N/n , t_s , and T_s will depend on the details of the atom-surface interaction. With suitable approximations these quantities can be estimated for surface relaxation involving adsorption and permeation of He³.

B. Adsorption-Controlled Relaxation

Helium is known to adsorb onto Pyrex surfaces

with an energy of adsorption $E \sim 0.01$ eV.¹⁸ Frenkel showed that the sticking time per collision is related to E by the expression $t_s = t_s^0 \times \exp(E/kT)$, where $t_s^0 \sim 10^{-13}$ sec.¹⁹ corresponding in the high-temperature limit to simple reflections of the incident gas atoms at the surface.

The number n of gas atoms adsorbed at any instant is just the product of t_s and the rate at which atoms strike the wall,

$$n = (N\bar{v}A/4V)t_s,$$

where \bar{v} is the mean thermal velocity of the He³ atoms, V the sample volume, and A the surface area. Note that A is not necessarily the geometric surface area but the area participating in the nuclear-spin relaxation. In this sense, A will depend on the surface density of relaxation sites as well as the microscopic "shape" of the glass boundary.

This work provides very little information about the relaxation time T_s for adsorbed atoms. Relaxation is presumably induced by paramagnetic centers on or near the container surface, but their nature, density, and locations relative to the surface are unknown. However, because t_s is so short ($\leq 10^{-12}$ sec) at the temperatures of interest, it is reasonable to expect that $\gamma\bar{H}_l t_s \ll 1$, where $\gamma = 2 \times 10^4$ rad sec⁻¹ G⁻¹ is the He³ nuclear gyromagnetic ratio and \bar{H}_l is the effective rms local magnetic field at the surface. In this limit, $(\gamma\bar{H}_l t_s)^2$ is just the probability W of a nuclear spin flip per encounter with the surface, and $T_s = t_s/(2W) \gg t_s$.²⁰

Substituting the expressions for T_s , t_s , and n into Eq. (4), the He³ adsorption-controlled relaxation time T_{1A} is given by

$$T_{1A} = 2Ve^{-2E/kT}/A\bar{v}(\gamma\bar{H}_l t_s^0)^2, \quad (5)$$

since $T_s \gg t_s$. (Note that the opposite limit, $T_s \ll t_s$, leads independently of T_s , to $T_{1A} = 2V/A\bar{v}$, in qualitative disagreement with the experimental behavior described in Sec. III.)

Though the spin-spin relaxation time T_{2A} was experimentally inaccessible, it is important to note that in the limit $\gamma\bar{H}_l t_s \ll 1$, T_{2A} should in fact be equal to T_{1A} .²⁰ This is significant for possible nuclear gyroscope applications discussed in Sec. VI.

The form of Eq. (5) suggests that a plot of $\ln(T_{1A})$ versus $1/kT$ should be linear with slope $-2E$. In Fig. 6 the low-temperature Pyrex data are plotted in this manner; each of the three samples separately exhibit the predicted linear behavior. Averaging the slopes for the three cases, the adsorption energy is about 0.01 eV with an error of roughly 0.003 eV. This is in good agreement with the published experimental

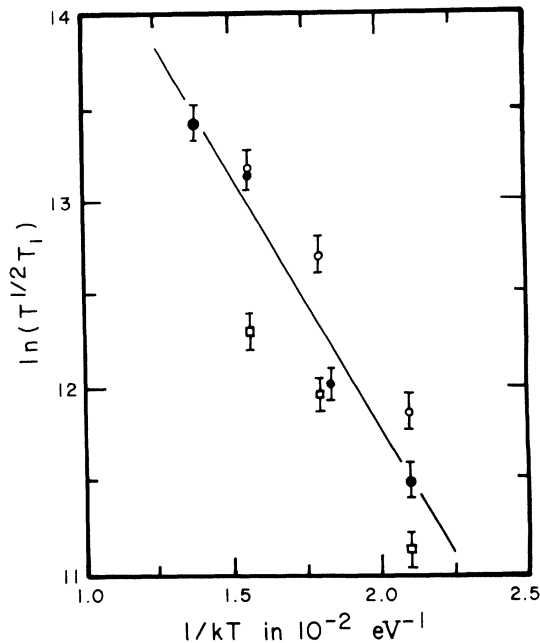


FIG. 6. Plot of $\ln(T^{1/2}T_1)$ versus $1/kT$ for the low-temperature Pyrex data. The solid, square, and circular points correspond to the data shown in Fig. 3, curves 1, 2, and 3, respectively. The solid line is a best fit to the data and corresponds to an adsorption energy of 0.01 eV for helium on Pyrex.

values for helium adsorption onto Pyrex.¹⁸

It is difficult to make numerical comparisons between experiment and theory because of the uncertainty associated with the surface area A , the local magnetic field \bar{H}_l , and t_S^0 . However, as an illustrative example, consider Pyrex containers at 77°K, for which $T_1 \sim 4 \times 10^6$ seconds. Assuming $t_S^0 = 10^{-13}$ sec and using the geometrical surface area, one finds that the rms local magnetic field at the surface would have to be of the order of 2.5 kG. A local field of this magnitude would imply that the glass surface is totally paramagnetic. While this can be regarded as a reasonable possibility, one might instead question the assumption of an effective relaxing area equal to the geometrical area. Micropores, fissures, and other surface irregularities could raise the effective area of the surface by a large factor, in which case a much reduced surface magnetic field would give agreement between theory and experiment.

A further complicating factor is the observed dependence of T_1 on the applied magnetic field. We are inclined to attribute this effect to field-dependent relaxation of the surface paramagnetic centers, reflected in Eq. (5) through \bar{H}_l . However, the field dependence of T_1 must in the last analysis remain an open question in the absence of any

better knowledge about the nature of the surface relaxing centers.

The surface-induced nuclear-spin relaxation for He^3 contained in aluminosilicate glass is adsorption-controlled for all accessible temperatures. A plot of $\ln(T^{1/2}T_1)$ versus $1/kT$ of the aluminosilicate data (curve 6 of Fig. 4) is shown in Fig. 7. In this case the resulting curve appears to be the composite of two linear parts, suggesting an interpretation in terms of two kinds of adsorption sites with adsorption energies of 0.1 and 0.01 eV, respectively. Equation (5) can easily be generalized to include two (or more) types of adsorption sites, and a two-site model with reasonable effective areas can be made to fit the data of Fig. 7. Though the fit is not unique because there are too many unknown parameters, the compatibility of the phenomenological model with the experimental data is nevertheless established.

C. Permeation-Controlled Surface Relaxation

It is well known that at moderate temperatures helium readily permeates fused quartz and glasses of high SiO_2 content. The maximum in the surface-induced He^3 relaxation time at about 125°K and its rapid decline at higher temperatures for quartz and Pyrex surfaces suggest the onset of a permeation-controlled relaxation mechanism.²¹ The solubility of helium, as well as its permeation and diffusion characteristics, have been estab-

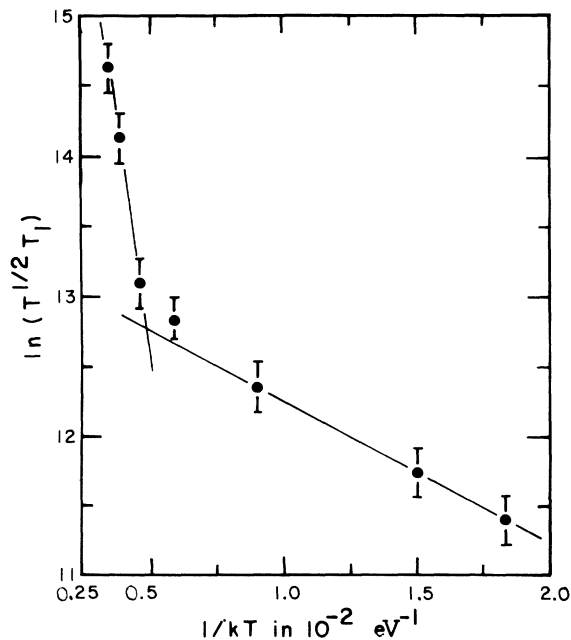


FIG. 7. Plot of $\ln(T^{1/2}T_1)$ versus $1/kT$ for the aluminosilicate data shown in Fig. 4, curve 6. The two linear portions suggest an interpretation in terms of two kinds of adsorption sites.

lished by previous work and may be used to evaluate n and t_s in Eq. (4).^{15, 16}

As before, the rate at which atoms dissolved in the glass exchange with atoms impinging on the surface from the gas is n/t_s . In this case, n is identified as the number of atoms dissolved within an average diffusion jump distance $\langle \Delta x \rangle$ of the surface.

The characteristic exchange, or sticking, time in the assumed model is $t_s \sim \alpha\tau$, where τ is the mean time between diffusive jumps for a dissolved He³ atom, and $\alpha \sim 6$ is a geometric factor required because the dissolved He³ atoms may jump in directions other than toward the surface. τ and $\langle \Delta x \rangle$ are related through the known diffusion coefficient D of helium in the glass of interest, $D = \langle \Delta x^2 \rangle / 6\tau$. For diffusion with activation energy Q , $\tau = \tau_0 \exp(Q/kT)$, where τ_0 is a constant for a given glass.²²

The solubility S of helium in all the glasses used in the present experiments has been determined by previous workers.^{15, 16} S is characteristically temperature independent, suggesting that the heat of solution for helium is very low, and therefore that the activation energies for permeation and diffusion are approximately equal. The solubilities and diffusion activation energies for the glasses of interest are shown in Table II, as are the values of τ_0 for an assumed jump distance $\langle \Delta x \rangle$ of 5 Å.

In terms of S , the number of dissolved atoms within a diffusion jump distance of the surface is

$$n = SA\langle \Delta x \rangle NkT/V.$$

Substituting for n and t_s in Eq. (4) yields the expression for diffusion, or permeation, controlled relaxation,

$$T_{1P} = (V/A\langle \Delta x \rangle S kT) \left(T_s + \alpha \tau_0 e^{Q/kT} \right), \quad (6)$$

where $t_s = \alpha\tau_0 \exp(Q/kT)$ and T_s is the characteristic nuclear-spin relaxation time for the He³ atoms dissolved in the glass. For this case, the relative values of T_s and t_s are uncertain. It is nevertheless tempting to attribute the rapid decline of T_1 above 125°K, observed for Pyrex and fused quartz surfaces, to the exponential term in the expression for T_{1P} . Indeed, the much short-

er relaxation times observed for fused quartz in comparison to Pyrex surfaces are consistent with the greater permeability of quartz to helium. This possible interpretation can be explored by assuming $T_s \ll t_s$, and plotting $\ln(TT_{1P})$ versus $1/kT$ to extract a value for Q . The result for Pyrex is a straight line yielding $Q \sim 0.05$ eV, which is about 5.5 times less than the reported diffusion activation energy for helium in Pyrex.¹⁶ This may reflect the fact that reported values of Q are characteristic of diffusion through the bulk glass, while it is predominantly diffusion within a few atomic distances of the surface that determines T_{1P} . Since the glass surface may reasonably be expected to have chemical composition and structural properties that are somewhat different from the bulk material, a different activation energy for diffusion is not surprising.

On the other hand, the assumption that $T_s \ll t_s$ is certainly open to question, particularly in view of the observed magnetic field dependence of T_1 for Pyrex surfaces at high temperatures shown in Fig. 5. For example, for Pyrex surfaces at 300°K, $T_1 \sim 6 \times 10^3$ sec. Assuming a diffusion jump distance of 5 Å, and that A is the geometrical area,

$$T_1(n/N) = (T_s + t_s) \approx 2.3 \times 10^{-6} \text{ sec.}$$

For this jump distance, $t_s \sim 3.3 \times 10^{-7}$ sec, implying that the permeation relaxation mechanism is dominated by the atom-surface relaxation time T_s . Here, however, the assumption that A is the geometrical area is questionable. If $T_s \gg t_s$, one must attribute the observed temperature dependence of T_{1P} to T_s [i. e., $T_s \sim \exp(Q/kT)$]. Holcomb and Norberg²³ have shown that this is in fact the expected relationship for diffusion-controlled nuclear relaxation in solids provided that $\omega_0\tau \gg 1$, where ω_0 is the nuclear Larmor frequency in the combined applied and local magnetic fields.

Thus the present data are insufficient to distinguish between the limiting cases $T_s \ll t_s$ or $T_s \gg t_s$, and little can be said about the spin-spin relaxation time T_{2S} . As in the adsorption-controlled relaxation limit discussed previously, explanation of the magnetic field dependence of T_1 must await a more detailed understanding of the surface paramagnetic centers responsible for He³ nuclear-spin relaxation.

TABLE II. Solubilities S , diffusion activation energies Q , and estimated τ_0 for glasses studied.

	Quartz (SiO ₂)	Pyrex 7740	Aluminosilicate 1723 1720	
S (He atoms/cm-Torr)	3.5×10^{14}	2.0×10^{14}	5.6×10^{13}	•••
Q (eV)	0.21	0.28	0.52	0.52
τ_0 (sec) for $\langle \Delta x \rangle = 5 \text{ \AA}$	7.5×10^{-11}	7.5×10^{-11}	•••	•••

V. RUBIDIUM OPTICAL-PUMPING EXPERIMENT

Bouchiat, Carver, and Varnum first reported the polarization of He³ gas by spin exchange with optically pumped rubidium vapor.¹¹ In their experiments the spin-exchange time was estimated to be between 10⁵ and 10⁶ sec. However, even though the polarization of the rubidium vapor was reported to be about 10%, only 0.01% He³ nuclear polarization was realized because the surface-induced He³ nuclear-spin relaxation time of about 2×10³ sec short-circuited the polarization process.

In terms of the electronic polarization P_{Rb} produced by optically pumping the rubidium vapor, the expected He³ ground-state polarization P_{He^3} can be expressed in terms of the Rb-He³ spin-exchange time τ_{ex} and the He³ nuclear-relaxation time T_1 .^{24,12}

$$P_{\text{He}} = P_{\text{Rb}} (1 + \tau_{\text{ex}}/T_1)^{-1},$$

where $\tau_{\text{ex}} = (\sigma_{\text{ex}} \bar{v} N_{\text{Rb}})^{-1}$, σ_{ex} is the He³ - Rb spin-exchange cross section reported by Gamblin and Carver²⁵ to be about 10⁻²⁴ cm², \bar{v} is the average collisional velocity in the center-of-mass system, and N_{Rb} is the rubidium atomic density. Using the rubidium polarization and characteristic times τ_{ex} and T_1 quoted by Bouchiat *et al.*,¹¹ and by Gamblin and Carver²⁵ the He³ polarization is predicted to be about 0.01%; i. e., the observed value. It is clear that sizeable He³ polarization cannot be expected unless T_1 is of the order of τ_{ex} . The time characterizing the polarization growth is $(1/\tau_{\text{ex}} + 1/T_1)^{-1}$.

In view of the long He³ nuclear-spin relaxation times observed for the aluminosilicate containers, a preliminary study was undertaken to determine if this method of optical pumping could be used to obtain significant polarization in high-density samples of He³ gas. A sample of He³ at 500 Torr was prepared in a Corning 1723 container by the procedures outlined previously. A small quantity of rubidium of natural isotopic content was distilled into the bulb prior to sealing. The bulb was placed in a nylon insulating chamber provided with Pyrex windows, and hot air was passed through the chamber to control the temperature. The optical pumping was accomplished with circularly polarized 7948 Å rubidium resonance radiation incident upon the sample through the Pyrex windows.

Optical pumping was performed in an axial magnetic field of about 6 G and the He³ polarization was monitored by NMR at 225 G by the method previously discussed. Measurements were made for a sample temperature of 100°C. At this temperature the spin exchange time is estimated to be 7×10⁶ sec. After 4 days (~4×10⁵ sec) of pumping the He³ polarization was about 0.5% and

still increasing approximately linearly with time. Pumping was then terminated (because of pumping lamp failure), and the polarization decay time (T_1) was measured to be about 9×10⁵ sec. Under the experimental conditions, and at a He³ density corresponding to a pressure of 500 Torr at room temperature, gradient relaxation effects are negligible.¹³ The intrinsic spin relaxation time resulting from nuclear dipole-dipole interactions during collisions in He³ gas is reliably estimated to be about 4×10⁷ T^{1/2}p⁻¹, where T is the absolute gas temperature and p the density expressed in units equal to the sample pressure in Torr at room temperature.²⁰ This expression gives an intrinsic relaxation time of roughly 1.5×10⁶ sec for this sample, very close to the measured relaxation time. The rubidium in the sample apparently has no adverse effect on the surface-induced nuclear-spin relaxation time.

Despite the uncertainty in P_{Rb} and the fact that the polarization experiment was not carried to completion, it is apparent that the He³ polarization attainable in aluminosilicate containers will be substantially larger than the values reported for samples contained in Pyrex. This technique holds considerable promise for the practical realization of dense polarized (~10%) He³ targets for nuclear- and high-energy scattering experiments.

VI. CONCLUSIONS AND DISCUSSION

The experimental results on surface-induced He³ nuclear spin-lattice relaxation are adequately described by the phenomenological model of Sec. IV, and provide strong evidence that there are at least two mechanisms - adsorption and permeation - by which He³ nuclei are retained in the vicinity of the glass container surfaces where they are relaxed by paramagnetic centers of an unknown nature.

A significant result of this work is the demonstration of the very long He³ spin relaxation times realizable at room temperature and above for samples contained in impermeable aluminosilicate glass. The longest relaxation time measured was 9×10⁵ sec (~9 days) at 100°C for a sample of 500-Torr pressure at room temperature. This is approximately equal to the intrinsic bulk relaxation time expected for that temperature and pressure. It is not unreasonable to expect that in a sufficiently homogeneous magnetic environment He³ spin relaxation times of months to years, characteristic of the bulk gas at lower densities, can be achieved at moderate temperatures in containers relatively impermeable to helium. The spin-lattice and spin-spin relaxation times should be identical under these circumstances. Such long relaxation times, combined with the very large He³ nuclear-spin polarization that can be produced by optical pumping, suggest the possible

application of spin-polarized gaseous He³ samples in experiments requiring very low friction gyroscopes (e.g., tests of general relativity,²⁶ and the search for a He³ nuclear dipole moment²⁷).

The feasibility of using the rubidium vapor optical-pumping technique to obtain a dense polarized He³ nuclear target has been demonstrated. Rubidium has no apparent adverse effect on surface-induced He³ nuclear-spin relaxation, and preliminary experiments suggest that sizeable He³ nuclear polarization (approaching the polar-

ization of the optically pumped rubidium vapor) might be attainable at He³ densities corresponding to several atmospheres pressure at room temperature.

VII. ACKNOWLEDGMENTS

We would like to thank Dr. L. L. Hatfield for helpful discussions and for assistance with the experiments. Helium for the low-temperature measurements was provided by the Office of Naval Research.

[†]Supported in part by the U. S. Atomic Energy Commission. Based on part of a Ph. D. thesis submitted by W. A. Fitzsimmons to Rice University, 1968.

*National Aeronautics and Space Administration Fellow in Physics. Present address: Physics Department, The University of Wisconsin, Madison, Wisconsin.

[‡]Present address: Physics Department, Stanford University, Stanford, California.

¹M. Bouchiat, *J. Phys. Radium* **24**, 379 (1963).

²H. C. Berg, *Phys. Rev.* **137**, A1621 (1965).

³E. Erb, J. L. Mochane, and J. Uebersfeld, *Compt. Rend.* **246**, 2121 (1958).

⁴J. Korringa, D. O. Seevers, and H. C. Torrey, *Phys. Rev.* **127**, 1143 (1962).

⁵G. K. Walters, *Helium Three* (Ohio State University Press, Columbus, Ohio, 1960) p. 37.

⁶G. K. Walters, unpublished; N. S. VanderVen, Ph. D. thesis, Princeton University, 1962 (unpublished).

⁷K. Luszczynski, R. E. Norberg, and J. E. Opfer, *Phys. Rev.* **128**, 186 (1962).

⁸H. H. McAdams, *Phys. Rev.* **170**, 276 (1968).

⁹See W. A. Fitzsimmons and G. K. Walters, *Phys. Rev. Letters* **19**, 943 (1967), for a preliminary account of this work.

¹⁰The nuclear polarization for a spin- $\frac{1}{2}$ system is defined as $P = (N_+ - N_-) / N$, where N_+ and N_- are the densities of atoms in the states of magnetic quantum number $+\frac{1}{2}$ and $-\frac{1}{2}$, respectively.

¹¹M. A. Bouchiat, T. R. Carver, and C. M. Varnum, *Phys. Rev. Letters* **5**, 373 (1960).

¹²F. D. Colegrove, L. D. Schearer, and G. K. Walters, *Phys. Rev.* **132**, 2561 (1963).

¹³L. D. Schearer and G. K. Walters, *Phys. Rev.* **139**, A1398 (1965).

¹⁴R. L. Garwin and H. A. Reich, *Phys. Rev.* **115**, 1478 (1959).

¹⁵F. J. Norton, *J. Am. Ceram. Soc.* **36**, 90 (1953).

¹⁶V. O. Altemose, *J. Appl. Phys.* **32**, 1309 (1961).

¹⁷F. D. Colegrove, L. D. Schearer, and G. K. Walters, *Phys. Rev.* **135**, A353 (1964).

¹⁸D. Muller, *Z. Physik* **188**, 326 (1965).

¹⁹J. Frenkel, *Z. Physik* **26**, 117 (1924).

²⁰N. Bloembergen, *Nuclear Magnetic Relaxation* (W. A. Benjamin, Inc., New York, 1961).

²¹P. Cornaz has independently suggested that permeation is responsible for He³ relaxation by Pyrex surfaces at room temperature [*Phys. Letters* **1**, 123 (1963)].

²²R. M. Barrer, *Diffusion in and Through Solids* (Cambridge University Press, Cambridge, England, 1941).

²³D. F. Holcomb and R. E. Norberg, *Phys. Rev.* **98**, 1074 (1955).

²⁴H. G. Dehmelt, *J. Phys. Radium* **19**, 866 (1958).

²⁵R. L. Gamblin and T. R. Carver, *Phys. Rev.* **138**, A946 (1965).

²⁶L. I. Schiff, *Phys. Rev. Letters* **4**, 215 (1960).

²⁷L. I. Schiff, *Phys. Rev.* **132**, 2194 (1963).